Reduced density matrix and combined dynamics of electrons and nuclei

Yang Zhao, Satoshi Yokojima, and GuanHua Chen
Department of Chemistry, University of Hong Kong, Pokfulam Road, Hong Kong

(Received 11 February 2000; accepted 14 June 2000)

Nuclear dynamics is incorporated into an efficient density matrix formalism of electronic dynamics which has been applied to molecular systems containing thousands of atoms. The formalism for the combined dynamics of electrons and nuclei is derived from the Dirac–Frenkel variational principle. The single electron reduced density matrices and the Glauber coherent states are used for the electronic and nuclear degrees of freedom, respectively. The new formalism is applicable to simulate the dynamics of large molecular systems. As an illustration of its validity, the formalism is employed to calculate the electron and nuclei dynamics of hydrogen molecules. © *2000 American Institute of Physics.* [S0021-9606(00)30734-6]

I. INTRODUCTION

Recently a linear scaling method, the localized density matrix (LDM) method, was developed to simulate electronic dynamics of very large molecular systems containing thousands of atoms.[1–3] It is based on the time-dependent Hartree–Fock (TDHF) approximation, and follows the evolution of a single electron reduced density matrix in real time. It has been applied successfully to simulate linear optical response of electrons in polyacetylene oligomers, carbon nanotubes, and poly(*p*-phenylenevinylene) (PPV) aggregates.[1–9] In these calculations the nuclei are frozen, and thus the nuclear dynamics is not included. Since the simulation is carried out in time domain, it is natural to include the nuclear dynamics. The LDM simulation time step for the electronic dynamics is 0.01 to 0.1 fs while the time step is on the order of 0.1 fs for the Car–Parrinello method[10] and 0.1 to 1 fs for the force field molecular dynamics simulation.[11] It is thus desirable to include the nuclear motion in the LDM calculation.

Traditionally the dynamics of electrons and nuclei in molecular systems is treated within the Born–Oppenheimer (BO) or the adiabatic approximation in which the time scale of nuclear motion is assumed to be much longer than that of the electron motion. The nuclear motion is often computed with potential energy surfaces (PES) or force fields which are often obtained from *ab initio* calculations. Numerical simulations beyond the BO approximation are limited to small systems due to the requirement of expensive computational resources for the electronic degrees of freedom. The electron–nuclear dynamics (END) method has been applied to diatomic or triatomic molecules.[12–15] The electronic and nuclear wave functions are approximated by the single Slater determinants and fixed-width Gaussian wave functions, respectively. Other important contributions to the nonadiabatic dynamics include the surface-hopping approaches by Tully *et al.*[16] which serve as an alternative to methods of a single average nuclear path. Also proposed were semiclassical treatments of curve crossings in reaction dynamics by Miller *et al.*,[17] and applications of similar nature to the spin-boson problem and internal conversion processes by Stock.[18]

In this paper we propose a method for treating the electrons and nuclei simultaneously without assuming different time scales for electrons and nuclei or the BO approximation. We therefore do not have to resort to the PES or force field in the calculation of nuclear dynamics. Since the electronic degrees of freedom may be handled efficiently with the LDM method, it is expected that the new method may ultimately be used to simulate the electronic and nuclear dynamics of large complex molecular systems. We adopt a variational approach for the combined dynamics of electrons and nuclei. The equations of motion for the electronic and nuclear degrees of freedom may be derived *rigorously* from the exact Lagrangian using the Dirac–Frenkel variational principle.[19] Similar to the END method, Glauber coherent states which correspond to the fixed-width Gaussians in real space are adopted for the nuclear motion. To take advantage of the LDM treatment of electrons, the reduced density matrices, instead of the wave functions, are used to describe the electronic dynamics. In parallel to our developments of the LDM methods for fixed nuclei which started from rather simple Hamiltonians, the semiempirical Hamiltonian, the complete neglect of differential overlap in spectroscopy (CNDO/S),[20] is used as the first implementation to describe the dynamics of electrons and nuclei. We emphasize that the adoption of CNDO/S Hamiltonians are not essential to our approach, and extensions to include more sophisticated Hamiltonians such as PM3 and the density functional theory (DFT)[21] can easily be implemented as in the case of fixed nuclei.[3,8]

The paper is organized as follows. In Sec. II we introduce the Dirac–Frenkel variational principle which allows for dynamical descriptions of the electrons and nuclei in a single framework. Formal equations of motion are derived in their respective subspaces for a single-configurational ansatz in Sec. II A. The nuclear classical equations of motion are deduced from the time-dependent variational principle in the limit of small coherent state widths. Generalizations to include multiple configurations are discussed in Sec. II B. The new formalism may be used to simulate the combined dynamics of electrons and nuclei in complex molecular systems. As a first step towards that goal, we adopt the CNDO/S

Hamiltonian and simulate the dynamics of electrons and nuclei in hydrogen molecules. Results are reported in Sec. IV. Discussions are presented in Sec. V.

II. COMBINED ELECTRONIC AND NUCLEAR DYNAMICS

The Dirac–Frenkel variational principle[19] is a powerful technique to obtain approximate dynamics for quantum systems for which exact solutions are elusive. The formulation starts with the exact Lagrangian

$$L=\langle \phi^T(t)|\frac{i\hbar}{2}\frac{\overleftrightarrow{\partial}}{\partial t}-\hat{H}|\phi^T(t)\rangle, \tag{2.1}$$

where $\phi^T(t)$ is an ansatz for the full normalized wave function of a quantum system which hinges on parameters $\eta_m\,(m=1,2,3,...)$. Here η_m can be complex c numbers or trial wave functions of subsystems. In general, the Dirac–Frenkel variational principle[19] leads to

$$\frac{d}{dt}\left(\frac{\partial L}{\partial \dot{\eta}_m^\dagger}\right)-\frac{\partial L}{\partial \eta_m^\dagger}=0, \tag{2.2}$$

where $\eta_m^\dagger$ stands for the complex conjugate of η_m.

Below we apply the Dirac–Frenkel variational principle to a single-determinant ansatz and its multiconfigurational generalization.

A. Single-configurational ansatz

The TDHF equation for fixed nuclei can be derived from the Dirac–Frenkel variational principle.[19] The trial wave function $|\phi^{\mathrm{HF}}\rangle$ for an electronic system is a single Slater determinant composed of N single-particle orbitals. One associates a single-particle density matrix $\rho_{ij}(t)$ with $|\phi^{\mathrm{HF}}\rangle$

$$\rho_{ij}(t)=\langle \phi^{\mathrm{HF}}|a_j^\dagger a_i|\phi^{\mathrm{HF}}\rangle, \tag{2.3}$$

where $a_j^\dagger(a_i)$ creates (annihilates) an electron at the jth (ith) orbital. The density matrix $\rho_{ij}(t)$, as a projector onto the space spanned by occupied orbitals, characterizes the Slater determinant up to within a phase. This is easily seen by exchanging two orbitals in $|\phi^{\mathrm{HF}}\rangle$ which leaves $\rho_{ij}(t)$ unchanged but $|\phi^{\mathrm{HF}}\rangle$ with a negative sign. In Appendix A, we give a brief derivation of the equations of motion for the density matrix $\rho_{ij}(t)$.

To include nuclear motion, we generalize the trial wave function in the TDHF approximation to include the nuclear degrees of freedom:

$$|\phi^T\rangle=|\phi^{\mathrm{HF}}\rangle|\phi^N\rangle, \tag{2.4}$$

where the normalized single Slater determinant $|\phi^{\mathrm{HF}}\rangle$ is composed of N single-particle orbitals ϕ_i, and $|\phi^N\rangle$ represents a normalized nuclear wave function. The Lagrangian has the form

$$L=\frac{i\hbar}{2}\sum_i\left(\langle\phi_i|\dot{\phi}_i\rangle-\langle\dot{\phi}_i|\phi_i\rangle\right)+\frac{i\hbar}{2}\left(\langle\phi^N|\dot{\phi}^N\rangle-\langle\dot{\phi}^N|\phi^N\rangle\right)-\langle\phi^T|\hat{H}|\phi^T\rangle. \tag{2.5}$$

We consider a system with M nuclei and N electrons. The nuclear and electronic coordinates are labeled as $\mathbf{r}_n$ $(n=1,...,M)$ and $\mathbf{r}_i^e$ $(i=1,...,N)$, respectively. The energy expression takes the form

$$\begin{aligned}E&\equiv\langle\phi^T|\hat{H}|\phi^T\rangle\\&=\langle\phi^N|-\sum_n\frac{\hbar^2}{2M_n}\frac{\partial^2}{\partial\mathbf{r}_n^2}+V_{NN}(\{\mathbf{r}_n\})|\phi^N\rangle\\&\quad+\langle\phi^T|-\sum_i\frac{\hbar^2}{2m_i}\frac{\partial^2}{\partial\mathbf{r}_i^{e2}}+V_{ee}(\{\mathbf{r}_i^e\})|\phi^T\rangle\\&\quad+\langle\phi^T|V_{eN}(\{\mathbf{r}_n\},\{\mathbf{r}_i^e\})|\phi^T\rangle,\end{aligned} \tag{2.6}$$

where M_n are the atomic mass for the nth atom, m_i is the ith electron mass, and $V_{NN}(\{\mathbf{r}_n\})$, $V_{ee}(\{\mathbf{r}_i^e\})$, and $V_{eN}(\{\mathbf{r}_n\},\{\mathbf{r}_i^e\})$ are the nucleus–nucleus, electron–electron, and nucleus–electron interaction energies, respectively.

Below we discuss separately the electronic and nuclear equations of motion derived from the variational procedure.

1. The electronic equations of motion

Applying the time-dependent variational approach,

$$\frac{d}{dt}\left(\frac{\partial L}{\partial\langle\dot{\phi}_i|}\right)-\frac{\partial L}{\partial\langle\phi_i|}=0, \tag{2.7}$$

we obtain the equations for the electronic degrees of freedom:

$$i\hbar\dot{\rho}=[h',\rho], \tag{2.8}$$

where the Fock matrix h' is given by

$$h'|\phi_i\rangle=\frac{\partial E}{\partial\langle\phi_i|}. \tag{2.9}$$

The difference between h' and the usual Fock matrix h (cf. Appendix A) lies only in that h', being dependent on

$$\langle\phi^{\mathrm{HF}}|V_{ee}(\{\mathbf{r}_i^e\})+V_{eN}(\{\mathbf{r}_n\},\{\mathbf{r}_i^e\})|\phi^{\mathrm{HF}}\rangle, \tag{2.10}$$

changes with time as the nuclei move. In other words, quantities such as v_{ij} in Eq. (3.1) are now time dependent in h' as compared with h. So far basis orbitals have not been specified. Orbitals fixed in space are not suitable to describe dynamical chemical systems, which may require a large number of basis functions. One needs to consider basis orbitals $\{\phi_i(t)\}$ which move with the nuclei. Equations of motion for the density matrix in a moving basis is

$$\dot{\rho}_{ij}=(i\hbar)^{-1}\langle\phi_i(t)|[h',\rho]|\phi_j(t)\rangle-\rho_{ij}\langle\phi_i(t)|\frac{\partial|\phi_i(t)\rangle}{\partial\mathbf{r}_i}\cdot\mathbf{V}_i-\rho_{ij}\frac{\partial\langle\phi_j(t)|}{\partial\mathbf{r}_j}\cdot\mathbf{V}_j|\phi_j(t)\rangle, \tag{2.11}$$

where $\mathbf{r}_i$ and $\mathbf{V}_i$ are, respectively, the position vector and velocity of the nucleus on which the ith orbital resides. The details of derivation are given in Appendix B.

2. Nuclear dynamics as coherent states

The nuclear degrees of the freedom are treated within the same variational framework. For example, the formal equation of motion for $|\phi^N\rangle$ is derived from

$$\frac{d}{dt}\left(\frac{\partial L}{\partial\langle\dot{\phi}^N|}\right)-\frac{\partial L}{\partial\langle\phi^N|}=0. \tag{2.12}$$

From the energy expression of Eq. (2.6) one readily arrives at

$$i\hbar|\dot{\phi}^N\rangle=\left[-\sum_n\frac{\hbar^2}{2M_n}\frac{\partial^2}{\partial\mathbf{r}_n^2}+V_{NN}(\{\mathbf{r}_n\})+\langle\phi^{\mathrm{HF}}|V_{ee}(\{\mathbf{r}_i^e\})+V_{eN}(\{\mathbf{r}_n\},\{\mathbf{r}_i^e\})|\phi^{\mathrm{HF}}\rangle\right]|\phi^N\rangle. \tag{2.13}$$

$\langle\phi^{\mathrm{HF}}|V_{ee}(\{\mathbf{r}_i^e\})|\phi^{\mathrm{HF}}\rangle$ is dependent on $\{\mathbf{r}_n\}$ in many approximation schemes, and thus cannot be neglected in Eq. (2.13). In order to capture fully the time evolution of nuclear motion, some detailed form of $|\phi^N\rangle$ has to be specified, and corresponding equations of motion derived.

For the nuclear wave function, a convenient ansatz to use is the Glauber coherent state.[22] The coherent states are equivalent to the so-called frozen Gaussian wave packets[23] in the real space representation. Frozen Gaussian wave packets are robust in time evolution. In contrast, Gaussian wave packets with variant widths are often found to be problematic.[24,25] The coherent state is regarded as a quantum mechanical state which approaches a classical state when the width goes to zero.[22,26–28] In fact, in a harmonic potential the coherent state undergoes the same dynamics using classical mechanics as using quantum mechanics. As $\hbar$ tends to zero, the width of the coherent state vanishes, and the nuclei are reduced to classical particles localized in the phase space. This makes the coherent states especially suitable for modeling quasiclassical systems.

We approximate the nuclear wave function $|\phi^N\rangle$ with a coherent state:

$$|\phi^N\rangle=|\alpha(t)\rangle=\prod_{i=1}^{3N}|\alpha_i(t)\rangle, \tag{2.14}$$

where α_i $(i=1,...,3N)$ are complex parameters that characterize the motion of N nuclei along x, y, and z directions, and the coherent state $|\alpha_i(t)\rangle$ may be expressed in the site representation as

$$\langle x|\alpha_i(t)\rangle=\pi^{-1/4}\exp\left\{-\frac{1}{2}\left[\sqrt{\frac{M_i\omega_i}{\hbar}}x-\sqrt{2}\,\mathrm{Re}(\alpha_i(t))\right]^2+i\,\mathrm{Im}(\alpha_i(t))\left[\sqrt{\frac{2M_i\omega_i}{\hbar}}x-\mathrm{Re}(\alpha_i(t))\right]\right\}, \tag{2.15}$$

where ω_i is the characteristic frequency for ith degree of freedom which determines the width of the Gaussian wave packet.

The Lagrangian takes the form

$$L=\frac{i\hbar}{2}(\langle\phi^N|\dot{\phi}^N\rangle-\langle\dot{\phi}^N|\phi^N\rangle)-E'=\frac{i\hbar}{2}\sum_{i=1}^{3N}(\dot{\alpha}_i\alpha_i^*-\dot{\alpha}_i^*\alpha_i)-E' \tag{2.16}$$

with

$$E'=\langle\alpha|-\sum_n\frac{\hbar^2}{2M_n}\frac{\partial^2}{\partial\mathbf{r}_n^2}+V_{NN}|\alpha\rangle+\langle\alpha|\langle\phi^{\mathrm{HF}}|V_{ee}+V_{eN}|\phi^{\mathrm{HF}}\rangle|\alpha\rangle. \tag{2.17}$$

This follows from

$$\langle\alpha_i|\dot{\alpha}_i\rangle=-\frac{1}{2}\frac{d}{dt}(\alpha_i\alpha_i^*)+\langle\alpha_i|e^{-1/2|\alpha_i|^2}\dot{\alpha}_i b_i^\dagger e^{\alpha_i b_i^\dagger}|0\rangle=-\frac{1}{2}\frac{d}{dt}|\alpha_i|^2+\dot{\alpha}_i\alpha_i^*, \tag{2.18}$$

where $b_i^\dagger(b_i)$ is the creation (annihilation) operator for ith degree of freedom, and is defined as

$$b_i^\dagger=\sqrt{\frac{M_i\omega}{2\hbar}}q_i+\sqrt{\frac{\hbar}{2M_i\omega}}\frac{\partial}{\partial q_i}, \tag{2.19}$$

$$b_i=\sqrt{\frac{M_i\omega}{2\hbar}}q_i-\sqrt{\frac{\hbar}{2M_i\omega}}\frac{\partial}{\partial q_i}. \tag{2.20}$$

Equations of motion for the complex displacement α_i then assume the simple form

$$i\hbar\dot{\alpha}_i=\frac{\partial E'}{\partial\alpha_i^*}. \tag{2.21}$$

Here α_i is related to the average nuclear position $\langle q_i\rangle_t$ and momentum $\langle p_i\rangle_t$ for the ith nuclear degree of freedom by

$$\alpha_i=\sqrt{\frac{M_i\omega_i}{2\hbar}}\langle q_i\rangle_t+i\sqrt{\frac{1}{2\hbar M_i\omega_i}}\langle p_i\rangle_t \tag{2.22}$$

with M_i the corresponding mass.

To understand the physics of Eq. (2.21), one may assume harmonic potentials for nuclei, for which

$$E'=\sum_i(|\alpha_i|^2+1/2)\hbar\omega_i. \tag{2.23}$$

The parameters α_i follow the equation of motion:

$$i\hbar\dot{\alpha}_i=\hbar\omega_i\alpha_i. \tag{2.24}$$

Equation (2.24) is in fact the classical equation of motion for a harmonic oscillator if $\langle q_i\rangle_t$ and $\langle p_i\rangle_t$ are substituted by the corresponding classical quantities. This shall become clearer in the next subsection.

There can be many generalizations for the ansatz of a single coherent state for the nuclear dynamics. One generalization is a superposition of many coherent states which better captures the quantum nature of the nuclear motion.[29] When the corresponding electronic state is multiconfigurational, such a generalization becomes absolutely necessary. In Sec. II B as well as Appendices E and F, we discuss the scenario of a multiconfigurational ansatz with a multi-

coherent-state nuclear wave function. Elsewhere in the paper, we shall confine ourselves to the single coherent state.

3. Recovery of nuclear classical equations of motion

Here we show that the equations of motion given by the Dirac–Frenkel variational principle lead to classical nuclear dynamics in the limit of vanishing width of the Gaussian wave packets. We also derive the lowest order corrections. The site and momentum representations of the coherent state are listed in Appendix C. By using the identity

$$\frac{\partial}{\partial \alpha_i^*}=\frac{1}{2}\frac{\partial}{\partial \alpha_i'}+i\frac{1}{2}\frac{\partial}{\partial \alpha_i''}, \tag{2.25}$$

where

$$\alpha_i'=\mathrm{Re}(\alpha_i), \quad \alpha_i''=\mathrm{Im}(\alpha_i), \tag{2.26}$$

the equation of motion (2.21) becomes

$$\hbar\dot{\alpha}_i'=\frac{1}{2}\frac{\partial E'}{\partial \alpha_i''},$$

$$\hbar\dot{\alpha}_i''=-\frac{1}{2}\frac{\partial E'}{\partial \alpha_i'}. \tag{2.27}$$

One uses the momentum-space representation of the coherent states (cf. Appendix C) to evaluate the kinetic term in E', yielding

$$\langle \dot{q}_i\rangle_t=\frac{\langle p_i\rangle_t}{M_i}. \tag{2.28}$$

One then uses the site-space representation of the coherent states (cf. Appendix C) for the potential terms in E'. Assume the width of the Gaussian wave packets is small so that one can expand the potential near the mean value $\langle q_i\rangle_t$. To the second order in the Taylor expansion, one obtains

$$\langle \dot{p}_i\rangle_t=-\left(\frac{\partial E'}{\partial q_i}\right)_{\langle q_i\rangle_t}. \tag{2.29}$$

The width of the Gaussian wave packets enters the equation of motion if the potential is expanded to the fourth order in the vicinity of $\langle q_i\rangle_t$. The lowest order correction to Eq. (2.29) is quadratic in the wave packet width a_i

$$-\frac{\sqrt{2}a_i^2}{8\hbar}\left(\frac{\partial^3 E'}{\partial x_i^3}\right)_{x_i=\sqrt{2}\alpha_i'}, \tag{2.30}$$

where the dimensionless quantity x_i is related to the position q_i by

$$x_i=\sqrt{\frac{M_i\omega_i}{\hbar}}q_i, \tag{2.31}$$

and $a_i=\sqrt{\hbar/(M_i\omega_i)}$ gives the width of the coherent state. To the second order in the Taylor expansion of the potential near the mean value $\langle q_i\rangle_t$, the classical equations of motion are fully recovered. Quantum effects are presented by the third-order terms which are proportional to the width squared.

B. Multiconfigurational ansatz

A multiconfigurational ansatz which contains more than one Slater determinants may take the form

$$|\phi^T\rangle=\sum_m c_m|\phi_m^{\mathrm{HF}}\rangle|\phi_m^N\rangle, \tag{2.32}$$

where $|\phi_m^{\mathrm{HF}}\rangle$ are single Slater determinants for the electrons, $|\phi_m^N\rangle$ are the nuclear wave functions, c_m are the configuration coefficients, and the configurational index m runs from 1 to M. The trial state (2.32) includes the multiple-trajectory feature that the surface-hopping approach,[16] and recently, the full-multiple-spawning method,[44] attempt to reproduce. The fully quantum-mechanical state (2.32) avoids artificial drawbacks such as undesired coherence destruction of the surface-hopping method. Starting from a single electron–nuclear configuration, a system should evolve on a single potential surface, and no bifurcation of the nuclear trajectory should occur until a curve crossing or a transition region is reached. Then an additional electron–nuclear configuration is introduced to describe the appearance of the new electronic state. The corresponding time dependence of c_m, $|\phi_m^{\mathrm{HF}}\rangle$ and $|\phi_m^N\rangle$ can be derived from the Dirac–Frenkel variational principle. As two nuclear trajectories diverge, their overlap vanishes. We may neglect the interference between them. Each trajectory evolves virtually independently. In Appendix E we demonstrate how a multiconfigurational ansatz of the form (2.32) is handled in a time-dependent variational procedure.

The trial wave function (2.32) bears close resemblance to the Davydov ansatz for the lattice Holstein model (cf. Appendix F):[30,31]

$$|\Phi(t)\rangle=\sum_n \psi_n(t)B_n^\dagger|0\rangle_{\mathrm{ex}}\exp\left[\sum_q(\lambda_{nq}(t)b_q^\dagger-\mathrm{H.c.})\right]|0\rangle_{\mathrm{ph}}, \tag{2.33}$$

where the index n labels the lattice sites, $|0\rangle_{\mathrm{ex}}(|0\rangle_{\mathrm{ph}})$ is the vacuum state for both the exciton (phonon) degrees of freedom, $B_n^\dagger$ creates an exciton on site n, and $b_q^\dagger$ creates a phonon of frequency ω_q. For each electronic configuration $B_n^\dagger|0\rangle_{\mathrm{ex}}$, a unique lattice wave function is assigned. The time-dependent parameters $\psi_n(t)$ and $\lambda_{nq}(t)$ which characterize the Davydov ansatz can also be determined from the Dirac–Frenkel variational principle. Details of ensuing equations of motion are given in Appendix F.

The similarities between the two ansätze can be explored to better understand Eq. (2.32). Both ansätze attach a distinct nuclear wave function to an electronic configuration. For the lattice Holstein model, each configuration $(B_n^\dagger|0\rangle_{\mathrm{ex}})$ corresponds to a single exciton stationed on a specific lattice site. For Eq. (2.32), each configuration corresponds to a Slater determinant made of individual orbitals. The Holstein model, however, does not require changing electronic configurations to adapt to changes of the lattice wave functions. Because the number of distinct one-exciton configurations equals the number of lattice sites regardless of detailed information on lattice deformation. It is not true for the trial state (2.32). The individual orbitals of which the Slater determinants are composed change as the nuclei move.

III. THE CNDO/S HAMILTONIAN

In this section we adopt a specific Hamiltonian for the electronic degrees of freedom, and restrict ourselves to closed shell molecules. The semiempirical CNDO/S Hamiltonian[20,32] is employed to describe the electrons and nuclei in molecules. With the CNDO/S Hamiltonian as the approximate Hamiltonian, h'_{ij} takes the form

$$h'_{ij}=t_{ij}+2\delta_{ij}\sum_k v_{ik}\rho_{kk}-v_{ij}\rho_{ij}, \tag{3.1}$$

where δ_{ij} is Kroenecker delta, and v_{ij} is the Coulomb repulsion between two electrons at orbitals i and j. The CNDO/S model adopts the zero differential overlap (ZDO) approximation, and the total energy of closed shell electronic system may be classified into one-atom and two-atom terms:

$$E^{\mathrm{tot}}=\sum_n E_n+\sum_{n<m} E_{nm}, \tag{3.2}$$

where

$$E_n=2\sum_i^{i\in n}\rho_{ii}U_{ii}+\sum_{ij}^{i,j\in n}(2\rho_{ii}\rho_{jj}-\rho_{ij}\rho_{ji})\gamma_{nn}, \tag{3.3}$$

$$E_{nm}=\sum_i^{i\in n}\sum_j^{j\in m}(4\rho_{ij}\beta_{ij}-2\rho_{ij}^2\gamma_{nm})+\frac{Z_nZ_m}{r_{nm}}-P_{nn}V_{nm}-P_{mm}V_{mn}+P_{nn}P_{mm}\gamma_{nm}. \tag{3.4}$$

Various quantities in Eqs. (3.3) and (3.4) are defined as follows. U_{ii} is a one-center term defined as

$$U_{ii}=\langle i|-\tfrac{1}{2}\nabla_i^2-V_i|i\rangle, \tag{3.5}$$

where V_i is the potential of electron i from nuclei and core electrons. γ_{nm} is the average Coulomb repulsion energy between an electron in any valence atomic orbital of the nth atom and another in an orbital of the mth atom, and V_{nm} is the interaction energy of an electron in any valence orbital of nth atom with the core of mth atom. Z_n is the core charge (including the nucleus and inner shells) of the nth atom, ρ_{ij} is the usual one-electron density matrix, and P_{nn} is the total valence electron charge on the nth atom

$$P_{nn}=2\sum_i^{i\in n}\rho_{ii}. \tag{3.6}$$

The off-diagonal core matrix elements between atomic orbitals on different atoms are estimated by

$$\beta_{ij}=\beta^0_{nm}S_{ij}, \tag{3.7}$$

where S_{ij} the overlap integral, and β^0_{nm} is a parameter depending on the nature of atoms n and m. r_{nm} is the distance between two nuclei n and m.

The average interaction energy γ_{nm} was first calculated by Roothaan.[33] Various approximations of γ_{nm} were later proposed. For example, in the Nishimoto–Magata approximation,[34] γ_{nm} is estimated from the

$$\gamma_{nm}=e^2\left(\frac{2e^2}{\gamma_{nn}+\gamma_{mm}}+R_{nm}\right)^{-1}, \tag{3.8}$$

where γ_{nn} is the average on-site repulsion energy for atom n. If the internuclear distance R_{nm} is large (above 3.5 Å), γ_{nm} becomes the interaction between two charged spheres. In the opposite limit when the nuclei coincide, γ_{nm} reduces to the repulsion of two electrons on the same nucleus. These one-center γ_{nn} are approximated by the well-known method introduced by Pariser[35]

$$\gamma_{nn}=\tfrac{1}{2}(I_n+A_n), \tag{3.9}$$

where I_n and A_n are the valence state ionization potential and the electron affinity, respectively. Following the CNDO/2 method,[32] V_{nm} is approximated by $Z_m\gamma_{nm}$ neglecting the penetration effects in which electrons in an orbital of one atom penetrate the shell of another leading to net attraction.

The force acting on the nucleus of the nth atom can be calculated from

$$\mathbf{F}_n=-\nabla_n(E^{\mathrm{tot}}+V_{NN}). \tag{3.10}$$

To simplify our simulation, we set

$$\frac{\partial\rho}{\partial\mathbf{r}_n}\approx 0. \tag{3.11}$$

Thus

$$\mathbf{F}_n=-\nabla_n\sum_m^{m\neq n}E_{nm}-\nabla_nV_{NN}, \tag{3.12}$$

where ∇_n stands for the derivative with respect to the position vector $\mathbf{r}_n$ of nth nucleus. The reader is referred to Appendix D for details of the nuclear-force evaluation.

IV. HYDROGEN MOLECULE

To demonstrate the feasibility of our approach to capture complex dynamics of electrons and nuclei, we simulate the dynamics of a hydrogen molecule under an incident external electric field. The ground state for the hydrogen molecule is a symmetric state formed from the atomic 1s orbitals, and the excited state, on the other hand, corresponds to the antisymmetric configuration. Each simulation is composed of two runs. In the first run, the electronic ground state is obtained via a self-consistent-field (SCF) calculation, and the equilibrium nuclear configuration is generated by allowing the nuclei to relax from an arbitrary set of initial positions. The electronic relaxation is simultaneously carried out by the time domain LDM ground state calculation.[5] Since the purpose of this run is to achieve both electronic and nuclear equilibria, the nuclear kinetic energy is depleted rapidly for fast convergence. In the second run, the equilibrium nuclear configuration is adopted as the initial configuration, and the external field is applied to perturb the combined system of electrons and nuclei. A time-domain Gaussian profile is given to the external field with an adjustable width t_g. This provides an electronic excitation up to $\sim\hbar/t_g$. To achieve excitation at a specific frequency ω_e, an oscillating term $\exp(-i\omega_e t/\hbar)$ is added to the external field. Dissipative mechanisms are introduced to relax both the electronic and nuclear subsystems. The electronic system is relaxed via the phenomenological dephasing, while the nuclear system is dissipated with small fraction (~0.05%) of nuclear kinetic

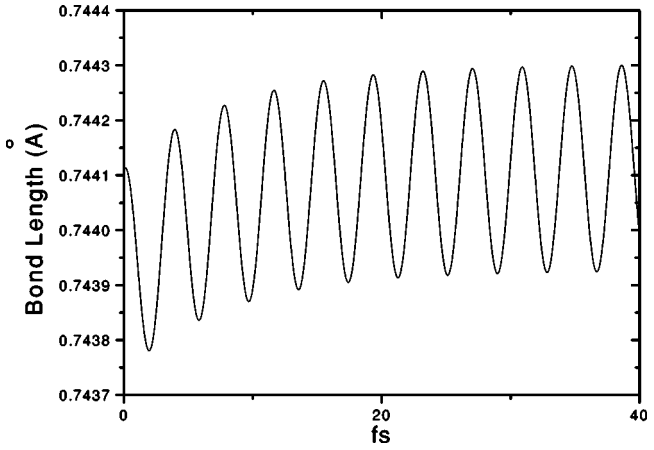

FIG. 1. H–H bond length of a hydrogen molecule with an external field. The field is applied at $t=0$ along the line connecting the two hydrogen atoms with an oscillating frequency of 18.54 eV. An electronic dephasing of 0.04 eV is adopted.

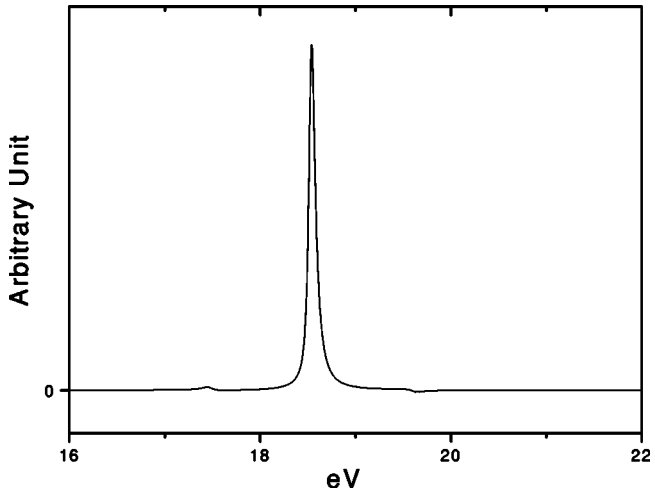

FIG. 3. The weak-field optical response of a hydrogen molecule: Im$[D(\omega)]$ versus ω, when $D(\omega)$ is the dipole moment of H_2. The field is applied along the line connecting the two hydrogen atoms. An electronic dephasing of 0.04 eV is adopted. The main peak is located at 18.54 eV.

energy taken out at each time step. Much weaker nuclear damping is adopted as compared with the first run in which 1–2 % of the nuclear kinetic energy is depleted per time step. Simulation is completed when the system recovers its initial state prior to the application of external field.

The time-evolution of the hydrogen–hydrogen bond length during the second run is displayed in Fig. 1. The field is applied along the line which connects the two hydrogen atoms so that no rotational motion is introduced. The electronic excitation disturbs the neutrality of the atoms causing a bond contraction in the first few femtoseconds. This is followed by bond oscillations with its mean gradually returning to equilibrium as the electronic excitation is dephased. The oscillation period is about 2.0 fs. Figure 2 shows the position displacement of one of the two nuclei in the second run. After the external field is applied, the nuclear movement exhibits a second oscillation with a much higher frequency. This is attributed to an electronic transition upon the external excitation which has an oscillating frequency of 18.54 eV. This in turn affects the nuclear movements. This high-frequency mode is absent in the bond length evolution shown in Fig. 1.

In Fig. 3 we plot the weak-field optical response of H_2. The vertical axis represents the value of Im$[D(\omega)]$, where $D(\omega)$ is the Fourier transform of H_2 dipole moment in the frequency domain. The electric field is weak so that the nuclei are only slightly disturbed. Clearly there is a peak at 18.54 eV which corresponds to the higher frequency oscillation in Fig. 2. The ground state of the hydrogen molecule is a symmetric bonding state while the excited state is a dissociative antibonding state. The energy gap between the ground state and the excited state is therefore represented by the peak at 18.54 eV. There are structures barely visible on the two sides which are phonon-induced and whose amplitudes strengthen upon increasing the external field. In Fig. 4 we display the strong-field optical response of the hydrogen molecule to a strong external field with a Gaussian packet

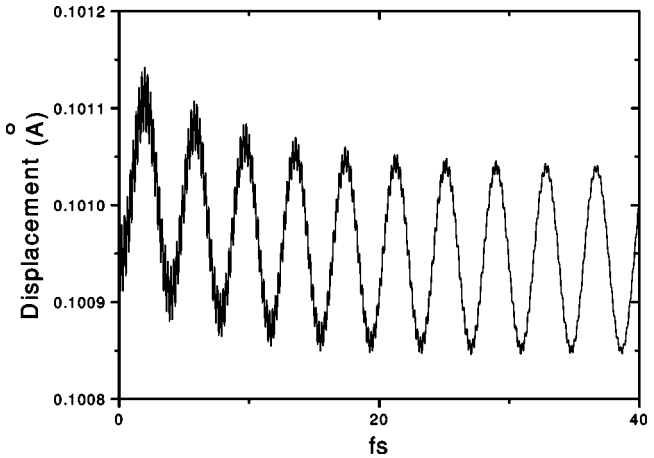

FIG. 2. Movement of one hydrogen atom driven by external field at 18.54 eV. The field is applied at $t=0$ along the line connecting the two hydrogen atoms with an oscillating frequency of 18.54 eV. An electronic dephasing of 0.04 eV is adopted.

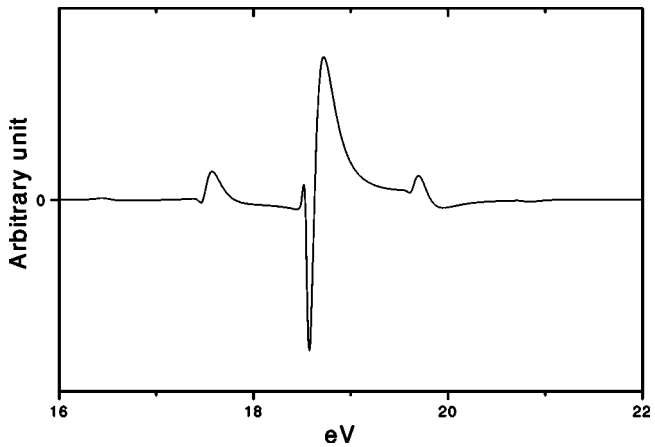

FIG. 4. The strong-field optical response of a hydrogen molecule: Im$[D(\omega)]$ versus ω. The field is applied along the line connecting the two hydrogen atoms. The time-domain width of the pulse is 0.1 fs. An electronic dephasing of 0.04 eV is adopted.

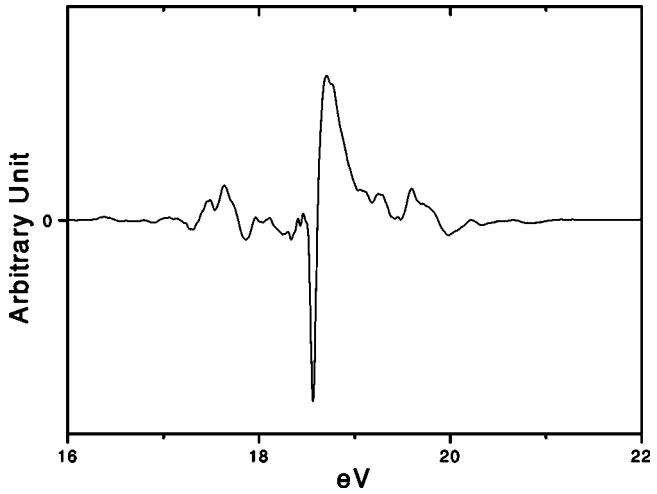

FIG. 5. Effect of collisions on the strong-field optical response of a hydrogen molecule. The time-domain width of the pulse is 0.1 fs. The characteristic collision time $1/\nu$ is 1 fs. The temperature for the Boltzmann distribution is 225 K.

width of 0.1 fs. There is a predominant structure at 18.54 eV. Phonon-induced features appearing on two sides are separated from the main structure by 1.1 eV which corresponds to the bond length oscillation frequency shown in Fig. 1.

In order to simulate a realistic system where atomic collisions frequently occur, we introduce a mechanism for energy fluctuations in which the temperature is kept constant.[36] A stochastic collision term is added to the equations of motion for nuclear dynamics. The resulting stochastic differential equations bear close resemblance to the Langevin equations for the Brownian motion.[37–39] Each stochastic collision is an instantaneous event which affects the momentum of one particle. The times at which different particles undergo collisions are statistically uncorrelated. The probability for the collision to take place between t and $t+dt$ is

$$p(t)dt=\nu\exp(-\nu t)dt, \tag{4.1}$$

where the characteristic collision time is $1/\nu$. Alternatively, one may state that the time intervals between two successive collisions are distributed according to $p(t)$. Therefore the probability for each individual atom to experience the next collision increases with time (counting from the previous collision)

$$\int_0^t p\,dt=1-\exp(-\nu t). \tag{4.2}$$

If a collision occurs, the momentum of the atom is replaced at random from a Boltzmann distribution at the temperature T

$$\frac{1}{(\sqrt{2\pi m k_B T})^3}\exp\left(-\frac{p_x^2+p_y^2+p_z^2}{2mk_BT}\right)dp_x\,dp_y\,dp_z. \tag{4.3}$$

The effect of collisions on the strong-field responses of a hydrogen molecule is shown in Fig. 5. The characteristic collision time $1/\nu$ in Eq. (4.1) is 1 fs. The temperature from which the Boltzmann distribution is drawn is 225 K. Apart from the added collision term, the system parameters are kept the same as those in Fig. 4. Compared with Fig. 4, the signs of the stochastic process are obvious in Fig. 5, although the basic features in Fig. 4 survives the collision effect.

V. DISCUSSION

We have developed a method for simulating the combined dynamics of electrons and nuclei in complex systems. The dynamics is described by the single reduced density matrices for electrons and the Glauber coherent states for nuclei. Since the linear-scaling LDM method may be used to simulate the electronic dynamics, the method opens up a wide range of applications and may be employed to calculate the combined dynamics of large complex systems.

The simulations run so far are mostly in the Born–Oppenheimer regime as the energy scale in the electronic system greatly exceeds that of the nuclear system, although nuclear movements on the same order of frequencies as the electrons are shown to exist under a high-frequency driving field. Our approach can be generally applied to nonadiabatic regimes where the two energy scales are comparable. Similar nonadiabatic methods with combined quantum and classical dynamics for electrons and nuclei were applied to scattering problems and small systems.[12,15,40] Determinantal wave functions[41,42] were used instead of density matrices for the electronic dynamics. These calculations were restricted only to small systems. In comparison, our approach has the potential to be applied to much larger systems. Generalizations to include multiple configurations and more sophisticated nuclear wave functions are also possible. In Appendix E we illustrate how nuclear and electronic wave functions are handled in a multiconfigurational ansatz.

The single-trajectory approach employed here belongs to the class of theories based on the time-dependent self-consistent-field method (TDSCF).[43] Compared with multiple-trajectory approaches such as the surface-hopping method[16,39] and the full-multiple-spawning algorithm,[44] nuclei follow an average mean path in TDSCF. Therefore TDSCF may not be a good approximation when the excited state acquires a significant population and its adiabatic potential surface greatly diverges from that of the ground state. Since in the cases examined here the excited state population is kept small at all times, the validity of our approach should hold.

The CNDO/S method gives a larger force constant than that is experimentally observed for the case of the hydrogen molecule (about twice too large, see Ref. 45). However, the purpose of our example is mainly to demonstrate the feasibility of our method instead of providing a close comparison with the experiments. Furthermore, as we have demonstrated for fixed nuclei, the simplified electronic Hamiltonian CNDO/S employed in this paper can be generalized to Hamiltonians of higher sophistication (for instance, PM3 and DFT) in order to better describe nuclear potential surfaces for complex molecules. We have previously extended our LDM calculations from CNDO/S Hamiltonians to PM3 Hamiltonians for fixed nuclei with ease.[7,8] We expect such extensions to include more sophisticated electronic Hamiltonians carried out for mobile nuclei in the next stage of developments.

Dynamics calculations in the literature often treat the environment of a quantum system classically.[46–48] Attempts were also made to infer absorption lineshapes from such hybrid calculations.[49] Our method which mixes the quantum electronic system with its classical nuclear environment is expected to capture quantities that have classical interpretations. These include time-dependent observables such as electronic populations and mean positions and momenta of vibrational modes. However, it is not able to reproduce the vibronic features in the absorption spectra. The failure is caused by inability of classical nuclear dynamics to describe the nuclear wave function overlaps at different times. Although the full quantum vibronic spectra are not reproduced with the lattice treated classically, peaks at $\omega_{eg} \pm n\omega_{\text{nuclear}}$ (n is an integer) are observed from the hybrid simulations, albeit often with negative signs. It is understood as a lattice perturbation to the electronic transition. The signs of the peaks shall depend on the relative phase between the electronic and nuclear oscillations as demonstrated by the simple identities:

$$2\sin x \sin y = -\cos(x+y) + \cos(x-y), \tag{5.1}$$

$$2\sin x \cos y = \sin(x+y) + \sin(x-y), \tag{5.2}$$

$$2\cos x \cos y = \cos(x+y) + \cos(x-y). \tag{5.3}$$

From the first identity, the two peaks at $\omega_{eg} \pm \omega_{\text{nuclear}}$ will have opposite signs, while from the last two identities, the peaks will have the same sign. We point out that the optical response shown in Figs. 3 and 4 are not absorption spectra. The coupled equations of motion for electrons Eq. (2.11) and nuclei with the nuclear force given by Eq. (3.12) are not expanded in terms of the external electric field and thus the optical responses we obtained include linear and nonlinear components.

In our model the nuclear motion can be viewed as a classical bath that is coupled to the electronic degrees of freedom. The combined system of electrons and nuclei therefore serves as a paradigm for chromophore-bath systems. If the nuclear motion is harmonic then the bath is bosonic. A simple anharmonic bath is a collection of two-level systems (TLS)[50] which are responsible for the chromophore transition frequency modulation in glasses. Strong anharmonicity is expected in the hydrogen molecule disturbed by a moderate external field. We have simulated the transfer of the electronic energy from the incident laser light into the nuclear (bath) system. It is found that such transfers in the hydrogen molecule require ~100 fs to complete after excitation by strong external pulses.

There have been studies of the simultaneous dynamics of electrons and nuclei in a linear monatomic chain and in a zig–zag chain of nitrogen atoms.[40] What constitutes a physically more interesting system are polymers such as polyacetylene and poly(*p*-phenylenevinylene). Polarons and solitons are among the different entities which emerge in those polymers.[51–58] Modern techniques of femtosecond spectroscopy[59] shall reveal, in details previously unavailable, the complex dynamics of electrons and nuclei in these materials. Since the polymers are flexible and can change its shape easily, spectroscopic properties of polymers depend heavily on nuclear motion. Most computations of the optical response of large polymers treat the nuclear effect phenomenologically because of the excessive computational cost to determine the PES. In comparison our method is not constrained by PES computations. The density-matrix formulation given here which can be readily incorporated into the LDM method is a computationally efficient tool to model combined dynamics of electrons and nuclei in large systems.

ACKNOWLEDGMENTS

Support from the Hong Kong Research Grant Council (RGC) and the Committee for Research and Conference Grants (CRCG) of the University of Hong Kong is gratefully acknowledged.

APPENDIX A: THE TIME-DEPENDENT HARTREE–FOCK APPROXIMATION

The TDHF equations can be derived from the time-dependent variational approach. First, one defines the Lagrangian

$$L = \langle \phi^T | \frac{i\hbar}{2} \frac{\overleftrightarrow{\partial}}{\partial t} - \hat{H} | \phi^T \rangle. \tag{A1}$$

Here the trial wave function $|\phi^T\rangle$ is a normalized single Slater determinant so that Lagrange multipliers are not needed. Equations of motion for the trial wave function $|\phi^T\rangle$ are obtained from

$$\frac{d}{dt}\left(\frac{\partial L}{\partial \langle \dot{\phi}_i|}\right) - \frac{\partial L}{\partial \langle \phi_i|} = 0, \tag{A2}$$

where $|\phi_i\rangle$ are the individual orbitals which make up the HF wave function. We then arrived at

$$-i\hbar|\dot{\phi}_i\rangle + \frac{\partial E}{\partial \langle \phi_i|} = 0 \tag{A3}$$

with

$$E \equiv \langle \phi^T | \hat{H} | \phi^T \rangle. \tag{A4}$$

The complex conjugate of Eq. (A3) has the form

$$i\hbar\langle\dot{\phi}_i| + \frac{\partial E}{\partial |\phi_i\rangle} = 0. \tag{A5}$$

Define the single-electron density matrix ρ as

$$\rho = \sum_i^{\text{occ}} |\phi_i\rangle\langle\phi_i| \tag{A6}$$

and the Fock matrix h as

$$h|\phi_i\rangle = \frac{\partial E}{\partial \langle \phi_i|}. \tag{A7}$$

From (A7), it is easy to show that h is a function of ρ. Thus, one readily obtains the closed equation of motion for ρ from Eqs. (A3) and (A5),

$$i\hbar\dot{\rho} = [h, \rho]. \tag{A8}$$

APPENDIX B: EQUATIONS OF MOTION IN A MOVING BASIS

Orbitals fixed in space are prone to convergence problems in the time evolution. To consider basis orbitals which move with the nuclei, we write the one-electron density matrix in terms of a time-dependent basis:

$$\rho=\sum_{ij}\ \rho_{ij}(t)|\phi_i(t)\rangle\langle\phi_j(t)|, \tag{B1}$$

where $|\phi_i(t)\rangle$ is the orbitals that centers on the moving nuclei. Then the equation of motion for $\rho_{ij}(t)$ follows:

$$\begin{aligned}(i\hbar)^{-1}[h',\rho]=\dot{\rho}=&\sum_{ij}\ \dot{\rho}_{ij}|\phi_i(t)\rangle\langle\phi_j(t)|\\&+\rho_{ij}\frac{\partial|\phi_i(t)\rangle}{\partial\mathbf{r}_i}\cdot\mathbf{V}_i\langle\phi_j(t)|\\&+\rho_{ij}|\phi_i(t)\rangle\frac{\partial\langle\phi_j(t)|}{\partial\mathbf{r}_j}\cdot\mathbf{V}_j,\end{aligned} \tag{B2}$$

where $\mathbf{r}_i$ and $\mathbf{V}_i$ are, respectively, the position vector and velocity of the nucleus on which the ith orbital resides. The individual elements of the density matrix therefore follows Eq. (2.11). The last two terms in Eq. (2.11) describe the difference between changes of ith and jth orbitals. In a hydrogen molecule, the two terms cancel each other. When the velocities of the nuclei are small, the two terms can be neglected in general.

APPENDIX C: COHERENT STATES IN SITE AND MOMENTUM REPRESENTATION

The coherent states in one dimension are related to the number states by

$$|\alpha\rangle=e^{-(|\alpha|^2/2)}\sum_{n=0}^{\infty}\frac{\alpha^n}{\sqrt{n!}}|n\rangle. \tag{C1}$$

In the site-space representation the number states are[60]

$$\langle x|n\rangle=2^{-(n/2)}\pi^{-(1/4)}\frac{1}{\sqrt{n!}}e^{-(x^2/2)}H_n(x), \tag{C2}$$

where $H_n(x)$ are the Hermite functions. The dimensionless quantity x is related to the position q_x by

$$x=\sqrt{\frac{M\omega}{\hbar}}q_x. \tag{C3}$$

The factor $\sqrt{M\omega/\hbar}$ determines the width of the Gaussian wave packet. Utilizing the identity

$$e^{-t^2+2tx}=\sum_{n=0}^{\infty}H_n(x)\frac{t^n}{n!}, \tag{C4}$$

one obtains the site-space expression of the coherent states

$$\begin{aligned}\langle x|\alpha\rangle=&\pi^{-(1/4)}\exp\{-\tfrac{1}{2}[x-\sqrt{2}\,\mathrm{Re}(\alpha)]^2\\&+i\,\mathrm{Im}(\alpha)[\sqrt{2}x-\mathrm{Re}(\alpha)]\}.\end{aligned} \tag{C5}$$

When α is real,

$$\langle x|\alpha\rangle=\pi^{-(1/4)}\exp\{-\tfrac{1}{2}[x-\sqrt{2}\,\mathrm{Re}(\alpha)]^2\}, \tag{C6}$$

which is a simply displaced ground state (the ''vacuum'' state $\phi_0=\pi^{-(1/4)}e^{-(1/2)x^2}$). The phase factor in Eq. (C5) is in fact the so-called ''electron translation factor'' which are usually multiplied to atomic orbitals to describe molecules in motion.

The momentum-space representation can be derived via a Fourier transform

$$\begin{aligned}\langle p|\alpha\rangle=&\frac{1}{\sqrt{2\pi}}\int dx\,e^{-ipx}\langle x|\alpha\rangle\\=&\pi^{-(1/4)}\exp\{-\tfrac{1}{2}[p-\sqrt{2}\,\mathrm{Im}(\alpha)]^2\\&-i\,\mathrm{Re}(\alpha)[\sqrt{2}p-\mathrm{Im}(\alpha)]\},\end{aligned} \tag{C7}$$

where the dimensionless quantity p is related to the momentum p_x by

$$p=\frac{1}{\sqrt{\hbar M\omega}}p_x. \tag{C8}$$

Equations (C5) and (C7) are essential for the derivation of classical dynamics from the time-dependent variational approach in Sec. II A 3.

APPENDIX D: THE CNDO/S APPROXIMATIONS

The Slater-type basis functions are used in the CNDO/S calculations:

$$\chi_a(r,\theta,\phi)=\frac{(2\zeta_a)^{n_a+(1/2)}}{\sqrt{(2n_a)!}}r^{n_\alpha-1}\exp(-\zeta_a r)Y_{l_am}(\theta,\phi), \tag{D1}$$

where n_a, l_a, and m are the principal, azimuthal, and the magnetic quantum numbers, respectively, and $Y_{l_am}(\theta,\phi)$ is the real normalized spherical harmonics. ζ_a is the orbital exponent.

The overlap integral S_{ab} can be written in terms of the reduced overlap integral $s(n_a,l_a,m,n_a,l_b,\alpha,\beta)$:

$$\begin{aligned}&S_{ab}(n_a,l_a,m,n_b,l_b,\alpha,\beta)\\&\quad=\frac{\zeta_a^{n_a+(1/2)}\zeta_b^{n_b+(1/2)}}{\sqrt{(2n_a)!(2n_b)!}}s(n_a,l_a,m,n_a,l_b,\alpha,\beta)r_{ab}^{n_a+n_b+1},\end{aligned} \tag{D2}$$

where

$$\alpha=\zeta_a r_{ab},\quad \beta=\zeta_b r_{ab}, \tag{D3}$$

$$\begin{aligned}s(n_a,l_a,m,n_a,l_b,\alpha,\beta)=&D(l_a,l_b,m)\sum_{ij}\ C_{ij\lambda}\\&\times A_i\left(\frac{\alpha+\beta}{2}\right)B_j\left(\frac{\alpha-\beta}{2}\right).\end{aligned} \tag{D4}$$

Here $D(l_a,l_b,m)$ is a function of l_a, l_b, and m, and $C_{ij\lambda}$ are matrices labeled by λ which itself is a function of n_a, n_b, l_a, l_b, and m:

$$\lambda=\lambda(n_a,n_b,l_a,l_b,m). \tag{D5}$$

The auxiliary functions $A(x)$ and $B(x)$ are defined as

$$A_k(x)=e^{-x}\sum_{n=1}^{k+1}\frac{k!}{x^n(k-n+1)!}, \tag{D6}$$

$$B_k(x)=-A_k(x)-e^{x}\sum_{n=1}^{k+1}\frac{(-1)^{k-n}k!}{x^n(k-n+1)!}. \tag{D7}$$

From Eq. (D2), the derivative of the overlap integral S_{ab} with respect to r_{ab} is composed of two terms:

$$\frac{dS_{ab}}{dr_{ab}}=(n_a+n_b+1)\frac{S_{ab}}{r_{ab}}+\frac{\zeta_a^{n_a+(1/2)}\zeta_b^{n_b+(1/2)}}{\sqrt{(2n_a)!(2n_b)!}}\frac{ds}{dr_{ab}}r_{ab}^{n_a+n_b+1}, \tag{D8}$$

where

$$\frac{ds}{dr_{ab}}=D(l_a,l_bm)\sum_{ij}C_{ij\lambda}\left[\frac{dA_i\left(\frac{\alpha+\beta}{2}\right)}{dr_{ab}}B_j\left(\frac{\alpha-\beta}{2}\right)+A_i\left(\frac{\alpha+\beta}{2}\right)\frac{dB_j\left(\frac{\alpha-\beta}{2}\right)}{dr_{ab}}\right]. \tag{D9}$$

The internuclear forces may now be derived from the energy expressions developed:

$$\mathbf{F}_n=-\sum_{m}^{m\neq n}\frac{dE_{nm}}{dr_{nm}}\boldsymbol{\nabla}_n r_{nm}-\boldsymbol{\nabla}_n V_{NN}, \tag{D10}$$

where

$$\boldsymbol{\nabla}r_{nm}=\frac{\mathbf{r}_n-\mathbf{r}_m}{r_{nm}}, \tag{D11}$$

$$\frac{dE_{nm}}{dr_{nm}}=-\frac{Z_nZ_m}{r_{nm}^2}+\frac{dS_{nm}}{dr_{nm}}\sum_{i}^{i\in n}\sum_{j}^{j\in m}4\rho_{ij}\beta_{nm}^0+\frac{d\gamma_{nm}}{dr_{nm}}\left(P_{nn}P_{mm}-P_{nn}Z_m-P_{mm}Z_n+\sum_{i}^{i\in n}\sum_{j}^{j\in m}2\rho_{ij}^2\right). \tag{D12}$$

Here the derivative of the overlap integral S_{nm} with respect to $r_{nm}(dS_{nm}/dr_{nm})$ follows Eq. (D8).

In the remainder of this appendix we discuss some specifics of the hydrogen molecule. The one-electron density matrix is calculated from

$$\rho_{ij}=\sum_{\nu}^{\mathrm{oc}}c_{\nu i}c_{\nu j}, \tag{D13}$$

where $c_{\nu j}$ is the coefficients of expansion of the molecular orbitals in terms of the valence atomic orbitals. Greek indices are used to denote the molecular orbitals. For the case of the hydrogen molecule, all elements of the ground state density matrix equal $\frac{1}{2}$. The total molecular energy for H_2 in the CNDO/2 approximation has the form

$$E^T=-(I+A)_{\mathrm{H}}-\frac{1}{2}\gamma_{\mathrm{HH}}-2\beta_{\mathrm{HH}}^0S_{\mathrm{HH}'}-\frac{3}{2}V_{\mathrm{HH}'}+\frac{1}{R_{\mathrm{HH}'}}, \tag{D14}$$

where I_{H} and A_{H} are the ionization potential and electron affinity of hydrogen, respectively. For two hydrogen atoms, $\gamma_{\mathrm{HH}'}$ has the form[33]

$$\gamma_{\mathrm{HH}'}=\frac{\zeta}{\rho}\left[1-\left(1+\frac{11}{8}\rho+\frac{3}{4}\rho^2+\frac{1}{6}\rho^3\right)e^{-2\rho}\right], \tag{D15}$$

where ζ is the orbital exponent, $\rho=\zeta R_{\mathrm{HH}'}$. The above expression for $\gamma_{\mathrm{HH}'}$ is different from the Nishimoto–Magata approximation. The difference in their derivatives with respect to the nuclear separation $R_{\mathrm{HH}'}$ is even greater. Adopting the Nishimoto–Magata approximation therefore results in less accurate equilibrium bond lengths. To remedy the problem, we add a proportionality constant (on the order of 1–2) to the second term on the right-hand side of Eq. (D12) calculating the forces so that the experimental values of the bond lengths are reproduced.

APPENDIX E: A MULTICONFIGURATIONAL ANSATZ

In this appendix we show how the nuclear and electronic trial wave functions are handled in a multiconfigurational ansatz in one space dimension. The ansatz has the form

$$|\phi^T\rangle=\sum_{m}c_m|\phi_m^{\mathrm{HF}}\rangle|\phi_m^N\rangle, \tag{E1}$$

where $|\phi_m^{\mathrm{HF}}\rangle$ are single Slater determinants for the electrons, $|\phi_m^N\rangle$ are the nuclear wave functions, c_m are the configuration coefficients, and the configurational index m runs from 1 to M. We need to introduce in the variation a Lagrange multiplier λ to ensure

$$N=\langle\phi^T|\Phi^T\rangle=\sum_{mn}c_n^*c_m\langle\phi_n^{\mathrm{HF}}|\phi_m^{\mathrm{HF}}\rangle\langle\phi_n^N|\phi_m^N\rangle=1. \tag{E2}$$

From

$$\frac{d}{dt}\left(\frac{\partial L}{\partial\dot{c}_k^*}\right)-\frac{\partial L}{\partial c_k^*}=\lambda\frac{\partial N}{\partial c_k^*}, \tag{E3}$$

we give the equations of motion for c_m,

$$-i\hbar\sum_{m}\left[\dot{c}_mI_{mk}+c_m(\langle\phi_k^N|\phi_m^N\rangle\langle\phi_k^{\mathrm{HF}}|\dot{\phi}_m^{\mathrm{HF}}\rangle+\langle\phi_k^{\mathrm{HF}}|\phi_m^{\mathrm{HF}}\rangle\times\langle\phi_k^N|\dot{\phi}_m^N\rangle)\right]+\frac{\partial E}{\partial c_k^*}=\lambda\sum_{m}c_mI_{mk}, \tag{E4}$$

where

$$E=\langle\phi^T|\hat{H}|\phi^T\rangle, \tag{E5}$$

$$I_{mk}=\langle\phi_k^{\mathrm{HF}}|\phi_m^{\mathrm{HF}}\rangle\langle\phi_k^N|\phi_m^N\rangle. \tag{E6}$$

Including Eq. (E2), there are altogether $M+1$ equations for $M+1$ variables (c_k and λ).

Next, assuming the nuclear wave functions take the coherent state form

$$|\phi_n^N\rangle=|\alpha_n\rangle, \tag{E7}$$

we derive the nuclear part of the equations of motion from

$$\frac{d}{dt}\left(\frac{\partial L}{\partial\dot{\alpha}_m^*}\right)-\frac{\partial L}{\partial\alpha_m^*}=\lambda\frac{\partial N}{\partial\alpha_m^*}. \tag{E8}$$

Utilizing

$$\langle \alpha_n|\alpha_m\rangle = \exp(\alpha_n^*\alpha_m - \tfrac{1}{2}|\alpha_m|^2 - \tfrac{1}{2}|\alpha_n|^2), \tag{E9}$$

$$\langle \alpha_n|\dot{\alpha}_m\rangle = \exp(\alpha_n^*\alpha_m - \tfrac{1}{2}|\alpha_m|^2 - \tfrac{1}{2}|\alpha_n|^2) \times\left(-\frac{1}{2}\frac{\partial}{\partial t}|\alpha_m|^2 + \alpha_n^*\dot{\alpha}_m\right), \tag{E10}$$

$$\langle \dot{\alpha}_n|\alpha_m\rangle = \exp(\alpha_n^*\alpha_m - \tfrac{1}{2}|\alpha_m|^2 - \tfrac{1}{2}|\alpha_n|^2) \times\left(-\frac{1}{2}\frac{\partial}{\partial t}|\alpha_n|^2 + \dot{\alpha}_n^*\alpha_m\right), \tag{E11}$$

one obtains the equations of motion for α_m:

$$i\hbar\dot{\alpha}_m = \frac{\partial(E-\lambda N)}{\partial\alpha_m^*} + \frac{i\hbar}{4}\sum_{n\neq m}\left[\alpha_m(\dot{K}_{nm}-\dot{K}_{mn}) - \frac{d}{dt}(2\alpha_n K_{nm})\right] - \frac{i\hbar}{2}\sum_{kn}\left[J_{kn}\frac{\partial\langle\alpha_n|\alpha_k\rangle}{\partial\alpha_m^*} - \frac{\partial K_{kn}}{\partial\alpha_m^*}\left(\frac{1}{2}\frac{d}{dt}|\alpha_k|^2 - \frac{1}{2}\frac{d}{dt}|\alpha_n|^2 + \alpha_n^*\dot{\alpha}_k - \dot{\alpha}_n^*\alpha_k\right)\right], \tag{E12}$$

where

$$J_{mn} = c_n^* c_m\langle\phi_n^{\mathrm{HF}}|\dot{\phi}_m^{\mathrm{HF}}\rangle + c_n^*\dot{c}_m\langle\phi_n^{\mathrm{HF}}|\phi_m^{\mathrm{HF}}\rangle - c_n^* c_m\langle\dot{\phi}_n^{\mathrm{HF}}|\phi_m^{\mathrm{HF}}\rangle - \dot{c}_n^* c_m\langle\phi_n^{\mathrm{HF}}|\phi_m^{\mathrm{HF}}\rangle, \tag{E13}$$

$$K_{mn} = c_n^* c_m\langle\phi_n^{\mathrm{HF}}|\phi_n^{\mathrm{HF}}\rangle\langle\phi_n^N|\phi_m^N\rangle. \tag{E14}$$

We are now left with the derivation of the equations of motion for the electronic degrees of freedom. If the inner products of two Slater determinants $\langle\phi_n^{\mathrm{HF}}|\dot{\phi}_m^{\mathrm{HF}}\rangle$ are written as

$$\langle\phi_n^{\mathrm{HF}}|\dot{\phi}_m^{\mathrm{HF}}\rangle = \delta_{nm}\sum_i\langle\phi_i^m|\dot{\phi}_i^m\rangle + (1-\delta_{nm})\langle\phi_n^{\mathrm{HF}}|\dot{\phi}_m^{\mathrm{HF}}\rangle, \tag{E15}$$

where $|\phi_i^m\rangle$ is the individual orbitals making up $|\phi_m^{\mathrm{HF}}\rangle$, equations of motion for

$$\rho^k = \sum_i^{\mathrm{occ}}|\phi_i^k\rangle\langle\phi_i^k| \tag{E16}$$

can be obtained from

$$-i\hbar|\dot{\phi}_i^k\rangle + \frac{\partial(E+F-\lambda N)}{\partial\langle\phi_i^k|} - \frac{d}{dt}\left(\frac{\partial F}{\partial\langle\dot{\phi}_i^k|}\right) = 0 \tag{E17}$$

in a similar fashion as the single configuration case in Appendix A. Here

$$F = \frac{i\hbar}{2}\sum_{nm}(1-\delta_{nm})c_n^* c_m\langle\phi_n^N|\phi_m^N\rangle(\langle\phi_n^{\mathrm{HF}}|\dot{\phi}_m^{\mathrm{HF}}\rangle - \langle\dot{\phi}_n^{\mathrm{HF}}|\phi_m^{\mathrm{HF}}\rangle) + \frac{i\hbar}{2}\sum_{nm}c_n^* c_m\langle\phi_n^{\mathrm{HF}}|\phi_m^{\mathrm{HF}}\rangle(\langle\phi_n^N|\dot{\phi}_m^N\rangle - \langle\dot{\phi}_n^N|\phi_m^M\rangle) + \frac{i\hbar}{2}\sum_{nm}(c_n^*\dot{c}_m - \dot{c}_n^* c_m)\langle\phi_n^{\mathrm{HF}}|\phi_m^{\mathrm{HF}}\rangle \times\langle\phi_n^N|\phi_m^N\rangle. \tag{E18}$$

The equations of motion for ρ^m so obtained have the form

$$i\hbar\dot{\rho}^m = [h^m, \rho^m] \tag{E19}$$

with the generalized Fock operator h^m given by

$$h^m|\phi_i^m\rangle = \frac{\partial(E+F-\lambda N)}{\partial\langle\phi_i^m|} - \frac{d}{dt}\left(\frac{\partial F}{\partial\langle\dot{\phi}_i^m|}\right). \tag{E20}$$

The density matrix ρ^m has a one-to-one correspondence with the Slater determinant $|\phi_m^{\mathrm{HF}}\rangle$ up to a phase. This can be understood from Eq. (E16) in which $|\phi_i^k\rangle$ are the eigenstates (with eigenvalues 1 or 0) that diagonalize the density matrix. For a given density matrix, therefore, its diagonalization determines the molecular orbitals ϕ_i^m, with which a Slater determinant differing from $|\phi_m^{\mathrm{HF}}\rangle$ is constructed upon by a phase factor.

APPENDIX F: THE DAVYDOV ANSATZ

In this appendix we shall take, as an example, the Davydov ansatz to illustrate how a multiconfigurational trial wave function is applied in a time-dependent variational procedure. The Davydov ansatz

$$|\Phi(t)\rangle = \sum_n\psi_n(t)B_n^\dagger|0\rangle_{\mathrm{ex}}\exp\left[\sum_q(\lambda_{nq}(t)b_q^\dagger - \mathrm{H.c.})\right]|0\rangle_{\mathrm{ph}} \tag{F1}$$

is adopted for the Holstein Hamiltonian[29,30] also known as the molecular crystal model,

$$\hat{H} = \hat{H}^{\mathrm{ex}} + \hat{H}^{\mathrm{ph}} + \hat{H}^{\mathrm{ex-ph}}, \tag{F2}$$

$$\hat{H}^{\mathrm{ex}} = -J\sum_n B_n^\dagger(B_{n+1}+B_{n-1}), \tag{F3}$$

$$\hat{H}^{\mathrm{ph}} = \sum_q\hbar\omega_q b_q^\dagger b_q, \tag{F4}$$

$$\hat{H}^{\mathrm{ex-ph}} = g\sum_{nq}\hbar\omega_q(b_q^\dagger e^{-iqn} + b_q e^{iqn})B_n^\dagger B_n. \tag{F5}$$

Here J is the exciton transfer integral between nearest neighbor sites, and g is the diagonal exciton-coupling coupling strength. We define the Debye–Waller factor $S_{mn}(t)$ as

$$S_{mn}(t) = {}_{\mathrm{ph}}\langle 0|\exp\left[\sum_q(\lambda_{mq}^*(t)b_q - \mathrm{H.c.})\right] \times\exp\left[\sum_q(\lambda_{nq}(t)b_q^\dagger - \mathrm{H.c.})\right]|0\rangle_{\mathrm{ph}}, \tag{F6}$$

or alternatively,

$$S_{mn}(t) = \langle\Lambda_m(t)|\Lambda_n(t)\rangle, \tag{F7}$$

where

$$|\Lambda_n(t)\rangle = \exp\left[\sum_q(\lambda_{nq}(t)b_q^\dagger - \mathrm{H.c.})\right]|0\rangle_{\mathrm{ph}}. \tag{F8}$$

From Eq. (2.1) the Lagrangian is given by

$$L=\frac{i\hbar}{2}\sum_n\ (\dot{\psi}_n\psi_n^*-\dot{\psi}_n^*\psi_n)$$

$$+\frac{i\hbar}{2}\sum_{nq}\ |\psi_n|^2(\dot{\lambda}_{nq}\lambda_{nq}^*-\dot{\lambda}_{nq}^*\lambda_{nq})-H, \tag{F9}$$

where H is defined as

$$H\equiv\langle\Phi(t)|\hat{H}|\Phi(t)\rangle. \tag{F10}$$

From the Dirac–Frenkel variational principle, one arrives at

$$i\hbar\dot{\psi}_n+\frac{i\hbar}{2}\psi_n\sum_q\ (\dot{\lambda}_{nq}\lambda_{nq}^*-\dot{\lambda}_{nq}^*\lambda_{nq})=\frac{\partial H}{\partial\psi_n^*}, \tag{F11}$$

$$\frac{i\hbar}{2}|\psi_n|^2\dot{\lambda}_{nq}+\frac{i\hbar}{2}\frac{d}{dt}(|\psi_n|^2\lambda_{nq})=\frac{\partial H}{\partial\lambda_n^*}, \tag{F12}$$

where H is explicitly given by

$$H=-J\sum_n\ \psi_n^*(\psi_{n+1}S_{n,n+1}+\psi_{n-1}S_{n,n-1})$$

$$+\sum_{nq}\ \hbar\omega_q|\psi_n|^2(|\lambda_{nq}|^2+ge^{-iqn}\lambda_{nq}^*+ge^{iqn}\lambda_{nq}). \tag{F13}$$

After simplifications, one obtains

$$i\hbar\dot{\psi}_n=-J(\psi_{n+1}S_{n,n+1}+\psi_{n-1}S_{n,n-1})$$

$$-\psi_n\left[\frac{i\hbar}{2}\sum_q\ (\dot{\lambda}_{nq}\lambda_{nq}^*-\dot{\lambda}_{nq}^*\lambda_{nq})+\hbar\omega_q(|\lambda_{nq}|^2\right.$$

$$\left.+ge^{-iqn}\lambda_{nq}^*+ge^{iqn}\lambda_{nq})\right] \tag{F14}$$

and

$$i\hbar\psi_n\dot{\lambda}_{nq}=\hbar\omega_q\psi_n(\lambda_{nq}+ge^{-iqn})-J\psi_{n+1}S_{n,n+1}(\lambda_{n+1}-\lambda_n)$$

$$-J\psi_{n-1}S_{n,n-1}(\lambda_{n-1}-\lambda_n). \tag{F15}$$

[1] S. Yokojima and G. H. Chen, Phys. Rev. B **59**, 7259 (1999).
[2] S. Yokojima and G. H. Chen, Chem. Phys. Lett. **292**, 379 (1998).
[3] W. Z. Liang, S. Yokojima, and G. H. Chen, J. Chem. Phys. **110**, 1844 (1999).
[4] S. Yokojima and G. H. Chen, Chem. Phys. Lett. **300**, 540 (1999).
[5] S. Yokojima, D. H. Zhou, and G. H. Chen, Chem. Phys. Lett. **302**, 495 (1999).
[6] W. Z. Liang, S. Yokojima, D. H. Zhou, and G. H. Chen, J. Phys. Chem. A **104**, 2445 (2000).
[7] S. Yokojima, X. J. Wang, D. H. Zhou, and G. H. Chen, J. Chem. Phys. **111**, 10444 (1999).
[8] W. Z. Liang, X. J. Wang, S. Yokojima, and G. H. Chen (unpublished).
[9] W. Z. Liang, S. Yokojima, and G. H. Chen, J. Chem. Phys. **113**, 1403 (2000).
[10] R. Car and M. Parrinello, Phys. Rev. Lett. **55**, 2471 (1985).
[11] A. Rahman, in *Correlation Functions and Quasiparticle Interactions in Condensed Matter*, edited by J. W. Halley, NATO Advanced Study Institutes Series Vol. 35 (Plenum, New York, 1977).
[12] E. Deumens, A. Diz, R. Longo, and Y. Öhrn, Rev. Mod. Phys. **66**, 917 (1994).
[13] J. Morales, A. Diz, E. Deumens, and Y. Öhrn, J. Chem. Phys. **103**, 9968 (1995).
[14] J. Broeckhove, M. D. Coutinho-Neto, E. Deumens, and Y. Öhrn, Phys. Rev. A **56**, 4996 (1997).
[15] M. J. Field, J. Chem. Phys. **96**, 4583 (1992).
[16] J. C. Tully and R. K. Preston, J. Chem. Phys. **55**, 562 (1971); J. C. Tully, *ibid.* **93**, 1061 (1990); D. Kohen, F. H. Stillinger, and J. C. Tully, *ibid.* **109**, 4713 (1998).
[17] W. H. Miller and T. F. George, J. Chem. Phys. **56**, 5637 (1972); W. H. Miller and C. W. McCurdy, *ibid.* **69**, 5163 (1978); H.-D. Meyer and W. H. Miller, *ibid.* **70**, 3214 (1979); **71**, 2156 (1979).
[18] G. Stock, J. Chem. Phys. **103**, 1561 (1995); **103**, 2888 (1995).
[19] P. A. M. Dirac, Proc. Cambridge, Phil. Soc. **26**, 376 (1930); J. Frenkel, *Wave Mechanics* (Oxford University Press, Oxford, 1934).
[20] J. Del Bene and H. H. Jaffé, J. Chem. Phys. **48**, 1807 (1968); **48**, 4050 (1968).
[21] W. Kohn and L. J. Sham, Phys. Rev. **140**, A1133 (1965).
[22] R. J. Glauber, Phys. Rev. **131**, 2766 (1963).
[23] E. J. Heller, J. Chem. Phys. **62**, 1544 (1975); **65**, 4979 (1976); **75**, 2923 (1981).
[24] J. R. Reimers and E. J. Heller, J. Phys. Chem. **92**, 3225 (1988).
[25] V. Chernyak and S. Mukamel, J. Chem. Phys. **105**, 4565 (1996).
[26] C. W. Gardiner, *Handbook of Stochastic Methods* (Springer, Berlin, 1983).
[27] S. Carusotto, Phys. Rev. A **11**, 1397 (1975).
[28] C. M. Savage and D. F. Walls, Phys. Rev. A **32**, 2316 (1985).
[29] Y. Zhao, D. W. Brown, and K. Lindenberg, J. Chem. Phys. **107**, 3159 (1997); **107**, 3179 (1997); **106**, 2728 (1997); **106**, 5622 (1997).
[30] T. Holstein, Ann. Phys. (N.Y.) **8**, 325 (1959).
[31] A. S. Davydov, *Theory of Molecular Excitons* (Plenum, New York, London, 1971).
[32] J. A. Pople and G. A. Segal, J. Chem. Phys. **44**, 3289 (1966).
[33] C. C. J. Roothaan, J. Chem. Phys. **19**, 1445 (1951).
[34] K. Nishimoto and N. Mataga, Z. Phys. Chem., Neue Folge **12**, 335 (1957).
[35] R. Pariser, J. Chem. Phys. **21**, 568 (1953).
[36] H. C. Andersen, J. Chem. Phys. **72**, 2384 (1980).
[37] M. C. Wang and G. E. Uhlenbeck, Rev. Mod. Phys. **17**, 323 (1945).
[38] U. Weiss, *Quantum Dissipative Systems* (World Scientific, Singapore, 1993).
[39] K. Mølmer, Y. Castin, and J. Dalibard, J. Opt. Soc. Am. B **10**, 524 (1993); S. Stenholm, Quantum Semiclassic. Opt. **8**, 297 (1996); S. Stenholm and M. Wilkens, Contemp. Phys. **38**, 257 (1997); F. Webster, P. J. Rossky, and R. A. Friesner, Comput. Phys. Commun. **63**, 494 (1991).
[40] J.-L. Calais, E. Deumens, and Y. Öhrn, J. Chem. Phys. **101**, 3989 (1994); A. Pohl and J.-L. Calais, *ibid.* **102**, 3269 (1995).
[41] D. J. Thouless, Nucl. Phys. **21**, 225 (1960).
[42] E. Dalgaard, J. Chem. Phys. **72**, 816 (1980).
[43] R. B. Gerber, V. Buch, and M. A. Ratner, J. Chem. Phys. **77**, 3022 (1982).
[44] M. Ben-Nun and T. J. Martinez, J. Chem. Phys. **112**, 6113 (2000).
[45] G. Herzberg, *Molecular Spectra and Molecular Structure: Spectra of Diatomic Molecules* (Van Nostrand, Princeton, NJ, 1966).
[46] J. T. Muckerman, I. Rusinek, R. E. Roberts, and M. Alexander, J. Chem. Phys. **65**, 2416 (1976).
[47] A. Selloni, P. Carnevali, R. Car, and M. Parrinello, Phys. Rev. Lett. **59**, 823 (1987).
[48] G. Wahnström, B. Carmeli, and H. Metiu, J. Chem. Phys. **88**, 2478 (1988).
[49] K. Haug and H. Metiu, J. Chem. Phys. **95**, 5670 (1991); **97**, 4781 (1992).
[50] Y. Zhao, V. Chernyak, and S. Mukamel, J. Phys. Chem. A **102**, 6614 (1998).
[51] R. H. Friend, D. D. C. Bradley, and P. D. Townsend, J. Phys. D **20**, 1367 (1987).
[52] Z. G. Soos, S. Ramasesha, D. S. Galvão, and S. Etemad, Phys. Rev. B **47**, 1742 (1993).
[53] M. Yan *et al.*, Phys. Rev. Lett. **72**, 1104 (1994).
[54] H. A. Mizes and E. M. Conwell, Phys. Rev. B **50**, 11243 (1994).
[55] G. H. Gelinck, J. M. Warman, and E. G. J. Staring, J. Phys. Chem. **100**, 5485 (1996).
[56] Y. Shimoi and S. Abe, Phys. Rev. B **50**, 14781 (1994).
[57] B. Champagne, E. Deumens, and Y. Öhrn, J. Chem. Phys. **107**, 5433 (1997).
[58] W. Utz and W. Förner, Phys. Rev. B **57**, 10512 (1998).
[59] R. Kersting *et al.*, Phys. Rev. Lett. **70**, 3820 (1993); R. Kersting *et al.*, J. Chem. Phys. **106**, 2850 (1997).
[60] G. Arfken, *Mathematical Methods for Physicists* (Academic, San Diego, 1985).